Proc. Natl. Acad. Sci. USA
Vol. 92, pp. 2657–2661, March 1995
Biochemistry

Kinetics of hydrogen bond breakage in the process of unfolding of ribonuclease A measured by pulsed hydrogen exchange

(protein denaturation/NMR-amide proton exchange/unfolding transition state)

THOMAS KIEFHABER† AND ROBERT L. BALDWIN

Department of Biochemistry, Stanford Medical Center, Stanford, CA 94305-5307

Contributed by Robert L. Baldwin, December 14, 1994

ABSTRACT **A sensitive test for kinetic unfolding intermediates in ribonuclease A (EC 3.1.27.5) is performed under conditions where the enzyme unfolds slowly (10°C, pH 8.0, 4.5 M guanidinium chloride). Exchange of peptide NH protons (^{2}H–^{1}H) is used to monitor structural opening of individual hydrogen bonds during unfolding, and kinetic models are developed for hydrogen exchange during the process of protein unfolding. The analysis indicates that the kinetic process of unfolding can be monitored by EX1 exchange (limited by the rate of opening) for ribonuclease A in these conditions. Of the 49 protons whose unfolding/exchange kinetics was measured, 47 have known hydrogen bond acceptor groups. To test whether exchange during unfolding follows the EX2 (base-catalyzed) or the EX1 (uncatalyzed) mechanism, unfolding/exchange was measured both at pH 8.0 and at pH 9.0. A few faster-exchanging protons were found that undergo exchange by both EX1 and EX2 processes, but the 43 slower-exchanging protons at pH 8 undergo exchange only by the EX1 mechanism, and they have closely similar rates. Thus, it is likely that all 49 protons undergo EX1 exchange at the same rate. The results indicate that a single rate-limiting step in unfolding breaks the entire network of peptide hydrogen bonds and causes the overall unfolding of ribonuclease A. The additional exchange observed for some protons that follows the EX2 mechanism probably results from equilibrium unfolding intermediates and will be discussed elsewhere.**

A basic unanswered question about the mechanism of protein folding is whether partially unfolded intermediates exist on the unfolding pathways of small single-domain proteins. Experiments based on optical probes of folding show that secondary and tertiary structures unfold with the same kinetics and suggest that there are no unfolding intermediates (1–7). Molecular dynamics simulations (8–12) of unfolding indicate, however, that unfolding intermediates with some hydrogen bonds broken exist and resemble the refolding intermediates (13–16), whose existence is well established.

The study of unfolding intermediates provides a direct approach to the problem of whether there is a unique transition state and pathway of folding (17–20) or whether multiple pathways are used simultaneously. Unfolding starts from the native state, which is a unique well-characterized conformation. Refolding starts, on the other hand, from the unfolded protein, whose conformation is poorly understood and which may contain two or more refolding species, each with a distinct refolding pathway, because of slow *cis–trans* isomerization of prolyl peptide bonds in the unfolded protein and similar phenomena (7). In addition, refolding experiments are not suited to detecting any intermediates that occur after the rate-limiting step of folding. This space on the energy diagram is accessible only from unfolding experiments. It is generally thought that the rate-limiting step in folding occurs close to the native conformation (1–7). If this view is correct, then the study of unfolding intermediates could give the most informative results about the nature of the rate-limiting step, because any unfolding intermediates would occur close to this step.

We introduce an approach to investigate the structural changes that occur during protein unfolding by monitoring directly the kinetics of destabilization of individual hydrogen bonds involving backbone NH protons. Under conditions where unfolding is slow and exchange of solvent-exposed NH protons is fast [10°C, pH 8.0, 4.5 M guanidinium chloride (GdmCl)], the NMR hydrogen exchange method gives an instantaneous probe of the kinetics of hydrogen-bond breakage during unfolding. If hydrogen bonds are already broken before the transition state for unfolding is reached, the unfolding exchange rates of these protons should be faster than the overall unfolding rate observed with optical probes.

MATERIALS AND METHODS

Materials. Ribonuclease (RNase) A (type XII-A) (EC 3.1.27.5) was purchased from Sigma and was used without further purification. GdmCl (ultra pure) was from United States Biochemical. Concentrated GdmCl solutions were filtered with Millipore filters with a pore size of 0.29 μm. ^2H_2O (99.9% purity) was from Isotec (Miamisburg, OH). All other chemicals were reagent grade and were purchased from Merck.

Native RNase A was deuterated by repetitive heating to 65°C for 30 min in ^2H_2O, pH* 3.5 (uncorrected glass electrode reading), and subsequent lyophilization. After three heating/lyophilization cycles, no remaining peptide NH protons could be detected in one dimensional NMR spectra of the native protein.

CD Measurements. Unfolding kinetics detected by CD were measured under the same conditions as the unfolding-exchange experiments to allow direct comparison of the data. Native deuterated RNase A (in ^2H_2O, pH* 3.5) was diluted 10-fold into final conditions of 4.5 M GdmCl, 45 mM Tris · HCl, 90% (vol/vol) ^1H_2O, 10% ^2H_2O at pH 8.0 and 10°C. Under these conditions the unfolding equilibrium for RNase A is >99.5% on the side of the unfolded protein (the transition region is between 3 M and 4.2 M GdmCl; data not shown). Unfolding was monitored by the change in the CD signal at 222 nm and at 275 nm in a Jasco J720 spectropolarimeter. Protein concentrations were 10 μM and 70 μM, respectively. The kinetics were fitted to two different mechanisms. The fit to the sum of two first-order reactions [$A = A_1{}^*\exp(-k_1{}^*t) + A_2{}^*\exp(-k_2{}^*t)$] gives significantly better results than the fit to a single exponential decay [$(A = A_0{}^* \exp(-k^*t)$]. Data fitting was performed on a Macintosh Quadra 650 microprocessor

The publication costs of this article were defrayed in part by page charge payment. This article must therefore be hereby marked "*advertisement*" in accordance with 18 U.S.C. §1734 solely to indicate this fact.

Abbreviation: Gdm, guanidinium.

†Present address: Biozentrum der Universität Basel, Abteilung Biophysikalische Chemie, Klingelbergstrasse 70, CH-4056 Basel, Switzerland.

using the program KaleidaGraph (Synergy Software, Reading, PA).

Unfolding/Exchange Experiments. All steps of the unfolding/exchange experiments were performed at 10°C. Unfolding was initiated by diluting native deuterated RNase A (in ^2H_2O, pH* 3.5) 10-fold with 50 mM Tris·HCl/5.0 M GdmCl, pH 8.0 or pH 9.0, in H_2O for final unfolding conditions of 4.5 M GdmCl, 45 mM Tris·HCl, 90% ^1H_2O, and 10% ^2H_2O. After various times of unfolding/exchange, the reaction was quenched by diluting the reaction mixture 10-fold with 50 mM NaOAc, pH 3.9, for a resulting pH of 4.0 and a residual GdmCl concentration of 0.45 M. Under these conditions RNase A is known to fold rapidly (within seconds) into a conformation where the NH protons are protected from exchange. At the same time, exchange is very slow at pH 4 (relaxation times in the range of 1000 s). The samples were concentrated with an Amicon YM10 ultrafiltration membrane at 4°C and the solvent was subsequently changed to ^2H_2O, pH* 3.5, by using Centricon 10 microconcentration tubes. Exchange was quantified by collecting absolute mode (magnitude) ^1H–^1H COSY (two-dimensional spin-correlated) NMR spectra on a General Electric GN-500 Omega 500 spectrometer or on a Bruker 500 spectrometer, both operating at a proton frequency of 500.13 MHz at 30°C, pH* 3.5. The data were processed by using the program NDEE (Franz Hermann, University of Bayreuth). The assignments of the cross-peaks to individual amide protons were given (21, 22). Cross-peak heights were determined and normalized to the nonexchanging aromatic cross-peaks of Tyr-25. The kinetic exchange curves were fitted to a single first-order exponential curve [$A = A_0$*exp(-k*t)] by using the program KaleidaGraph.

KINETIC MODEL FOR THE UNFOLDING/EXCHANGE KINETICS

Hydrogen exchange during the kinetic process of unfolding may occur by either of the two standard exchange mechanisms, EX1 or EX2 (23, 24), or it may occur by both mechanisms simultaneously. The basic considerations are as follows (23–26): (*i*) The folded structure of a protein blocks exchange both by hydrogen bonding peptide NH protons and by limiting access of water to protons that are not hydrogen-bonded. (*ii*) Rapid conformational fluctuations occur that permit exchange and so does overall unfolding, followed by refolding; the rates of these processes may be fast compared to the chemical exchange steps. (*iii*) Chemical exchange is base catalyzed (above pH 3), so that comparisons between the rates of chemical exchange and conformational change are strongly pH dependent. These rate comparisons determine whether exchange follows the EX1 or the EX2 mechanism.

If A is a folded, exchange-resistant conformation and A is in equilibrium with the exchange-susceptible conformation B, so that exchange (B → C) takes place from B, then the exchange reaction can be written

$$A \underset{k_{21}}{\overset{k_{12}}{\rightleftharpoons}} B \overset{k_{23}}{\rightarrow} C. \qquad [1]$$

The exchange mechanism is EX1 (limited by the rate of opening) when the rate of closing (k_{21}), which stops exchange, and the rate of opening (k_{12}), which leads to exchange, are both slow compared with the rate of chemical exchange (k_{23}). Then the exchange rate (k_{HX}) is given by the rate of opening (23, 24).

$$k_{HX} = k_{12}\ (k_{12}, k_{21} \ll k_{23})\ (\text{EX1}). \qquad [2a]$$

The exchange mechanism is EX2 (limited by the fraction open) when the rate at which B is converted back to A (k_{21}) is fast compared with chemical exchange (k_{23}).

$$k_{HX} = \left(\frac{k_{12}}{k_{12} + k_{21}}\right) k_{23}\ (k_{21} >> k_{23})\ (\text{EX2}). \qquad [2b]$$

[This is the complete expression for EX2 exchange given originally (23, 24); in later articles the term ($k_{12} + k_{21}$) is often approximated by k_{21}.] In EX2 exchange k_{HX} is base catalyzed because k_{23} is base catalyzed. This operational test is used here to distinguish EX1 from EX2 exchange.

Unfolding rates monitored by direct optical probes like CD and fluorescence (k_{app}) are the sum of rate constants for the unfolding and the refolding reactions (27)

$$N \underset{k_{21}}{\overset{k_{12}}{\rightleftharpoons}} U \qquad [3a]$$

$$k_{app} = k_{12} + k_{21} \qquad [3b]$$

in which N and U represent native and unfolded molecules, respectively. Unfolding measured by EX1 hydrogen exchange and by optical probes will give different kinetics in cases where the rate of refolding contributes significantly to k_{app}: exchange specifically measures the unfolding step (k_{12}), whereas optical probes see the sum of the unfolding and refolding steps (k_{12} + k_{21}). This effect may be envisioned from the different nature of the two methods. EX1 hydrogen exchange "marks" all molecules that have been unfolded at least once, since exchange occurs instantaneously as soon as a molecule unfolds. Optical probes, in contrast, see just the ratio of native to unfolded molecules. They cannot distinguish between native molecules that have been unfolded previously and native molecules that have never been unfolded. Likewise, the unfolding kinetics measured by CD and by hydrogen exchange are different in unfolding conditions if proline isomerization after unfolding affects the unfolding kinetics. A specific example, applicable to RNase A, is considered in *Discussion*.

RESULTS

Unfolding Kinetics Monitored by CD. Fig. 1 shows the unfolding kinetics of RNase A in 4.5 M GdmCl at 10°C, pH* 8.0. The CD intensity is shown at each of two wavelengths: one monitors the secondary structure (222 nm, used to observe α-helices) and the other monitors tertiary structure (275 nm, used to observe buried tyrosine residues that are fixed in a magnetically asymmetric environment). The unfolding curves monitored at the two different wavelengths are identical, indicating that secondary structure and tertiary structure unfold in the same process. Both curves show the total amplitude that is expected from equilibrium transition curves, showing that no faster reactions occur in the dead time of mixing. These results are found generally in the unfolding reactions of small single-domain proteins, and they give rise to the view that there are no detectable unfolding intermediates (1–7). The observed unfolding kinetics can be fitted approximately to a single first-order reaction with a relaxation time of τ = 370 s. More accurate fits are achieved, however, when the curves are fitted to the sum of two exponentials with relaxation times τ_1 = 420 s and τ_2 = 65 s; the faster phase has an amplitude of only 13%. The presence of a second kinetic phase in unfolding is expected because of kinetic coupling between protein folding and the *cis–trans* isomerization reaction of proline residues; this has been observed previously for folding of RNase A (28, 29).

Hydrogen Exchange During Unfolding. Exchange during the kinetic process of unfolding is measured here by diluting the deuterated folded protein from ^2H_2O into ^1H_2O containing concentrated GdmCl, pH 8.0, at the start of unfolding. Then exchange is quenched at the desired time by dropping the pH to 4.0 and diluting the GdmCl so that refolding can occur. RNase A refolds to an exchange-resistant state within a few

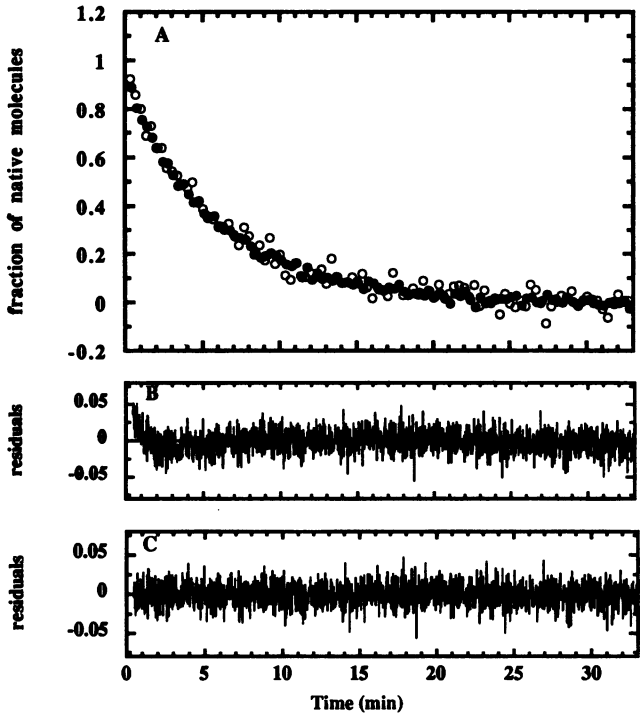

FIG. 1. (*A*) Unfolding of RNase A monitored by CD at two wavelengths: 222 nm (●) and 275 nm (○). Only part of the data points are shown. Unfolding conditions were pH 8.0, 10°C, 4.5 M GdmCl, 45 mM Tris·HCl. For comparison with the exchange experiments (Figs. 2 and 3) deuterated RNase A was used and the unfolding experiments were performed in 10% ^2H_2O/90% ^1H_2O. Protein concentrations were 10 and 70 μM for 222 and 275 nm, respectively. (*B*) Fitting the data to a single exponential curve gives a relaxation time $\tau = 370$ s. The residuals (222 nm) show a significant nonrandom pattern. (*C*) More accurate data analysis requires two exponentials with $\tau_1 = 420$ s (87% amplitude) and $\tau_2 = 65$ s (13% amplitude).

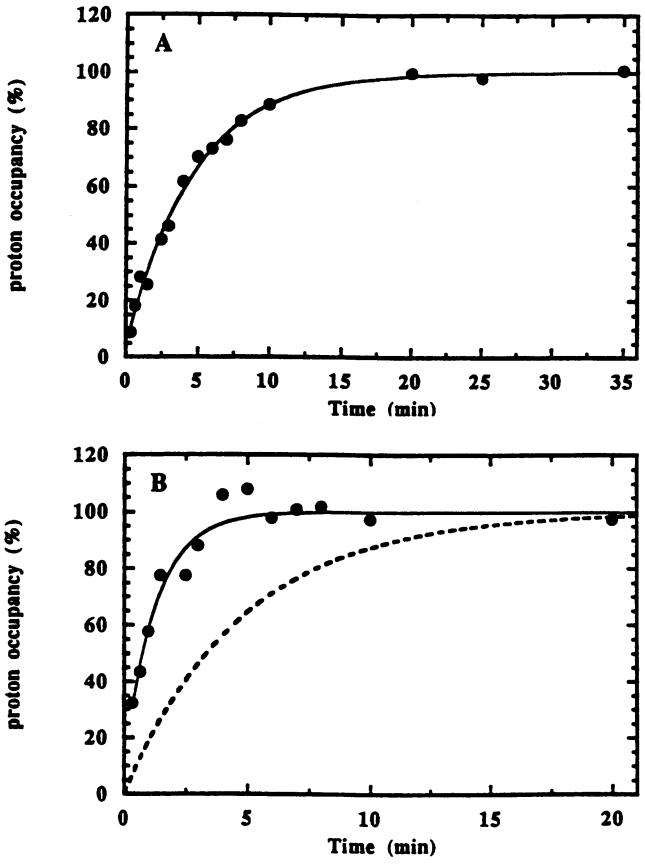

FIG. 2. Kinetic curves for hydrogen exchange during unfolding of deuterated RNase A for Val-63 (*A*) and for Val-124 (*B*). The broken line in *B* indicates the average exchange rate for the slow-exchanging protons. Unfolding conditions were pH 8.0, 10°C in 4.5 M GdmCl, 45 mM Tris·HCl, 10% ^2H_2O, 90% ^1H_2O. Unfolding exchange was quenched at the indicated times by lowering the pH to 4 (see *Materials and Methods*), where RNase A refolds rapidly to an exchange-resistant conformation. The amount of exchange was quantified by using two-dimensional spin-correlated spectra.

seconds (30). After the solvent has been changed to ^2H_2O, the two-dimensional NMR spectrum is recorded and the amount of exchange is quantified (see *Materials and Methods*). Representative kinetic curves for exchange during unfolding at pH 8.0 are shown in Fig. 2 for two individual protons: Val-63, which is a typical slow-exchanging proton, and Val-124, which is one of the fast-exchanging protons.

Curves as shown in Fig. 2 could be measured for 49 individual protons. Of these 49 protons, 47 have known hydrogen bond acceptors (22). The kinetic exchange curves show the following properties: (*i*) Unfolding/exchange can be fitted to a single exponential. There is no indication of a second, faster reaction, like the one observed in the CD kinetics, for any of the protons. (*ii*) The precision of measuring exchange rates is very good for slower-exchanging protons such as that of Val-63: the standard errors are in the range of 5–10%. (*iii*) Any initial burst or lag phase is small for all of the 49 resolved protons (note that the extent of exchange at time zero is known to be zero). The striking result for exchange at pH 8 (Fig. 3*A*) is that 43 of the 49 protons undergo unfolding/exchange at closely similar rates (the mean relaxation time is $\tau = 290$ s, with a standard deviation of $\sigma = 20$ s). The other six protons exchange with faster, but measurable, rates. Seven protons exchange too fast to measure.

To distinguish between pH-dependent and pH-independent unfolding/exchange, the experiments were repeated at pH 9.0 (Fig. 3*B*). At pH 9.0 the majority of the protons still exchange with a similar rate (the mean relaxation time is 230 s at pH 9, with $\sigma = 25$ s). The exchange rates of the six protons that are faster at pH 8 increase considerably at pH 9. The rates of two of those protons can still be measured at pH 9, while exchange of the four other protons becomes too fast to measure with manual mixing. An additional nine protons become significantly faster than the majority of the protons. None of the pH-dependent protons that can be measured at pH 9 shows the full 10-fold increase in rate expected for base catalysis. Thus, these protons undergo exchange by both the EX1 and EX2 mechanisms. Probably all protons show the same rate of exchange by the EX1 mechanism. If exchange by the EX1 and EX2 mechanisms occurs on parallel and independent pathways, then the observed exchange rate is the sum of the rates for the EX1 and EX2 processes.

The unfolding/exchange experiment at pH 8, 4.5 M GdmCl, has been repeated three times with nearly identical results, except that in the third experiment the pH seemed to be 0.1 pH unit lower, as judged from the reduced exchange rates of the pH-dependent protons. The third experiment is shown here; the exchange rates were measured with better precision in experiment 3 than in experiments 1 and 2 and in the pH 9 experiments because more time points were taken.

DISCUSSION

CD vs. Hydrogen Exchange Kinetics. A straightforward explanation for the difference in unfolding rates measured by CD and by hydrogen exchange follows from the fact that hydrogen exchange measures directly the unfolding rate constant k_{12}, while CD measures an apparent rate constant that

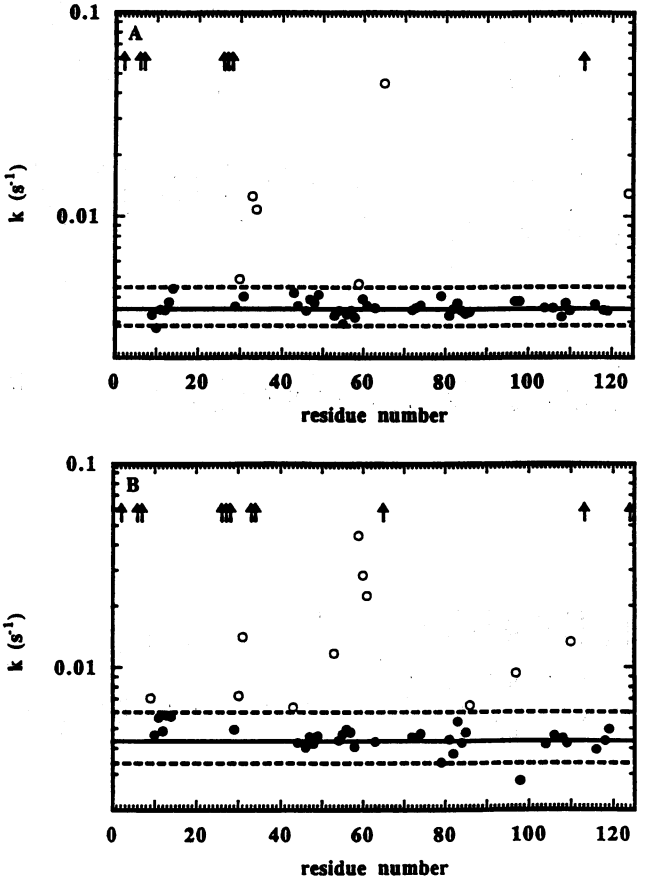

FIG. 3. Unfolding/exchange rates for the individual protons plotted against residue number at pH 8.0 (*A*) and pH 9.0 (*B*). Filled circles show rates within ± 3σ (σ = average standard deviation) of the mean rate of the slower-exchanging protons (solid line), while open circles show measurably faster rates. The broken lines indicate the ± 3σ limits. Arrows show the location of protons whose exchange rates are too fast to measure. The anomalously slow rate of Lys-98 at pH 9.0 is also shown by a filled circle.

includes microscopic rate constants for unfolding and refolding and for proline isomerization. The following mechanism represents the unfolding of RNase A in conditions like these (28, 29). It has been extended here to included the hydrogen-exchange reactions; the exchanged forms are denoted by *.

$$N \underset{k_{21}}{\overset{k_{12}}{\rightleftharpoons}} U_F \underset{k_{tc}}{\overset{2k_{ct}}{\rightleftharpoons}} U_S^A \underset{2k_{tc}}{\overset{k_{ct}}{\rightleftharpoons}} U_S^B \qquad [4]$$
$$\downarrow k_{23} \qquad \downarrow k_{23} \qquad \downarrow k_{23}$$
$$U_F^* \qquad U_S^{A*} \qquad U_S^{B*}$$

Here U_F and U_S indicate fast- and slow-folding unfolded species and k_{ct} and k_{tc} are rate constants for *cis* → *trans* and *trans* → *cis* isomerization. RNase A contains two *cis*-proline residues, whose *cis* → *trans* isomerization after unfolding is known to be primarily responsible for the formation of the slow-folding species (28, 31, 32).

The kinetic mechanism above can be solved, and the result shows that three macroscopic rate constants should be observable in unfolding/refolding kinetics (28). For unfolding in or just after the region of the unfolding transition (where our unfolding kinetics were performed), only two of the three macroscopic rate constants have measurable amplitudes (28). This explains the biphasic kinetics observed in the CD measurements. Hydrogen exchange, in contrast, still measures only the unfolding rate constant k_{12} because hydrogen exchange is irreversible (the presence of 10% ^2H_2O has a minor effect on the apparent rate constant) and hydrogen exchange is much faster than the succeeding proline isomerization reactions. Both the folding (k_{21}) and the unfolding (k_{12}) rate constants are small compared with hydrogen exchange of peptides at pH 8 and pH 9, as are the rate constants for proline isomerization (these reactions have typical relaxation times of τ = 50 to 300 s at 10°C). Peptide NH protons will thus exchange instantaneously once they reach the U_F state. Consequently, the observed EX1 kinetics measure the rate of the actual unfolding step (k_{12}).

We simulated the unfolding kinetics of RNase A at 4.5 M GdmCl for the model above, using the solution given (28) for unfolding/refolding kinetics measured by optical probes. The unfolding data monitored by CD and by EX1 hydrogen exchange were analyzed by the model in Eq. **4**, using $k_{21} = 1/50$ s^{-1}, $k_{12} = 1/290$ s^{-1}, $k_{ct} = 1/60$ s^{-1}, and $k_{tc} = 1/300$ s^{-1} (which are typical values for proline isomerization), and the model was found to give exact agreement with the observed values for the unfolding rate constants and amplitudes observed by CD and hydrogen exchange. The model does not, however, predict the unfolding transition curve accurately: it predicts 14% N in these unfolding conditions. Other factors, such as the presence of two *trans*-proline residues, may be responsible.

An alternative explanation for the difference between the unfolding rates measured by CD and hydrogen exchange is that some global EX2 exchange process contributes to the rate measured by hydrogen exchange. This explanation is unlikely because such an EX2 process would be 10 times faster at pH 9 than at pH 8 and would be expected to make the unfolding/exchange kinetics much faster at pH 9. This is not observed. Another alternative explanation is that unfolding/exchange occurs when an unfolding intermediate is formed that has labile but intact hydrogen bonds, so that exchange occurs rapidly but CD does not yet detect unfolding. Subsequently CD detects the complete unfolding of this intermediate. This explanation is unlikely because it predicts a pronounced lag in the CD-detected kinetics of unfolding, and this is not observed.

Transition State for Unfolding. Our results indicate that the entire network of peptide hydrogen bonds breaks in the transition state for unfolding. This conclusion is based on (*i*) finding that the rates of unfolding/exchange by the EX1 mechanism are the same for all peptide NH protons, and (*ii*) finding that the relaxation time for EX1 unfolding/exchange is consistent with the CD-detected unfolding rate, once the effect of proline isomerization after unfolding is taken into account. This result is consistent with the standard interpretation by experimentalists (1–7) of unfolding as a two-state reaction, but it provides a much more sensitive test than has been made before. Our conclusion is surprising in comparison with molecular dynamics simulations of unfolding of various proteins (8–12), which predict that some peptide hydrogen bonds are broken before the transition state is reached. It is important now to repeat this unfolding/exchange experiment with other small proteins (*i*) to test whether the presence of disulfide bonds in RNase A is responsible for this high cooperativity of unfolding, and (*ii*) to test whether the CD-detected and exchange-detected kinetics of unfolding are the same for proteins in which proline isomerization does not affect the unfolding kinetics.

This paper is dedicated to Prof. Rainer Jaenicke in the year of his 65th birthday. We thank Jon Goldberg, Doug Laurents, Steve Mayo, Andy Robertson, and Franz Schmid for help and discussion and Franz Hermann for adapting the program NDEE to our needs. We thank Gunter Fischer for the use of his NMR instrument and Gerd Scherer for instrumental help. Our work was supported by National Institutes of Health Grant GM 19988. T.K. was a fellow of the Deutsche Forschungsgemeinschaft.

1. Segawa, S. & Sugihara, M. (1984) *Biopolymers* **23**, 2437–2488.
2. Kuwajima, K., Mitani, M. & Sugai, S. (1989) *J. Mol. Biol.* **206**, 547–561.

3. Chen, B. L., Baase, W. A. & Schellman, J. A. (1989) *Biochemistry* **28,** 691–699.
4. Jackson, S. E. & Fersht, A. R. (1991) *Biochemistry* **30,** 10428–10435.
5. Chen, X. & Matthews, C. R. (1994) *Biochemistry* **33,** 6356–6362.
6. Serrano, L., Matouschek, A. & Fersht, A. R. (1992) *J. Mol. Biol.* **224,** 805–818.
7. Schmid, F. X. (1992) in *Protein Folding*, ed. Creighton, T. E. (Freeman, New York), pp. 197–239.
8. Dagget, V. & Levitt, M. (1992) *Proc. Natl. Acad. Sci. USA* **89,** 5142–5146.
9. Mark, A. E. & van Gunsteren, W. F. (1992) *Biochemistry* **31,** 7745–7748.
10. Tirado-Rives, J. & Jorgensen, W. L. (1993) *Biochemistry* **32,** 4175–4184.
11. Caflisch, A. & Karplus, M. (1994) *Proc. Natl. Acad. Sci. USA* **91,** 1746–1750.
12. Li, A. & Daggett, V. (1994) *Proc. Natl. Acad. Sci. USA* **91,** 10430–10434.
13. Baldwin, R. L. (1993) *Curr. Opin. Struct. Biol.* **3,** 84–91.
14. Woodward, C. K. (1994) *Curr. Opin. Struct. Biol.* **4,** 112–116.
15. Jennings, P. A. & Wright, P. E. (1993) *Science* **262,** 892–896.
16. Itzhaki, L. S., Evans, P. A., Dobson, C. M. & Radford, S. E. (1994) *Biochemistry* **33,** 5212–5220.
17. Bryngelson, J. D. & Wolynes, P. G. (1989) *J. Phys. Chem.* **93,** 6902–6915.
18. Honeycutt, J. D. & Thirumalai, D. (1992) *Biopolymers* **32,** 695–709.
19. Sali, D., Bycroft, M. & Fersht, A. R. (1991) *J. Mol. Biol.* **220,** 779–788.
20. Baldwin, R. L. (1994) *Nature (London)* **369,** 183–184.
21. Robertson, A. D., Purisima, E. O., Eastman, M. A. & Scheraga, H. A. (1989) *Biochemistry* **28,** 5930–5938.
22. Rico, M., Bruix, M., Santoro, J., Gonzales, C., Meira, J. L., Nieto, J. L. & Herranz, J. (1989) *Eur. J. Biochem.* **183,** 623–638.
23. Hvidt, A. (1964) *C. R. Trav. Lab. Carlsberg* **34,** 299–317.
24. Hvidt, A. & Nielsen, S. O. (1966) *Adv. Protein Chem.* **21,** 287–386.
25. Englander, S. W. & Kallenbach, N. R. (1984) *Q. Rev. Biophys.* **16,** 521–655.
26. Woodward, C., Simon, I. & Tüchsen, E. (1982) *Mol. Cell. Biochem.* **48,** 153–160.
27. Moore, J. W. & Pearson, R. G. (1981) *Kinetics and Mechanism* (Wiley, New York), 3rd Ed.
28. Kiefhaber, T., Kohler, H. H. & Schmid, F. X. (1992) *J. Mol. Biol.* **224,** 217–229.
29. Kiefhaber, T. & Schmid, F. X. (1992) *J. Mol. Biol.* **224,** 231–240.
30. Udgaonkar, J. B. & Baldwin, R. L. (1990) *Proc. Natl. Acad. Sci. USA* **87,** 8197–8201.
31. Schultz, D. A., Schmid, F. X. & Baldwin, R. L. (1992) *Protein Sci.* **1,** 917–924.
32. Houry, W. A., Rothwarf, D. M. & Scheraga, H. A. (1994) *Biochemistry* **33,** 2516–2530.